Vascular Networks Within 3D Printed and Engineered Tissues

Daniel Sazer and Jordan Miller

Contents

Abstract

In order to scale benchtop tissue mimics into viable constructs of clinically relevant dimensions, these structures must contain internal vascular networks to support convective mass transport. Without vessels to support perfusion culture, encapsulated cells located farther than 200 μm from the outer surface of a construct will quickly die due to the diffusional limits of oxygen and small molecule nutrients. By endowing artificial tissues with hollow vessels, researchers have made exciting progress towards the longitudinal maintenance of cellular function in large, dense tissues. But the field currently lacks standardized platforms and protocols to fabricate highly vascularized constructs in a rapid and cost-effective manner, which has left the literature base to become crowded

D. Sazer (✉) · J. Miller
Department of Bioengineering, Rice University, Houston, TX, USA
e-mail: dws6@rice.edu; jmil@rice.edu

A. Ovsianikov et al. (eds.), *3D Printing and Biofabrication*, Reference Series in Biomedical Engineering, https://doi.org/10.1007/978-3-319-45444-3_23

with custom apparatus and diverse technical schemes. Here we highlight some promising, contemporary strategies for the vascularization of 3D printed and engineered tissues. We discuss the advantages and limitations of various fabrication platforms in the field, making note of desirable properties such as high spatial resolution, freely tunable 3D architecture, and the presence of discrete fluidic ports. With clinical targets in mind, this overview concludes with a brief survey of progress towards fluidic integration with the circulatory system in vivo.

1 Introduction

Evidence of human tissue replacement dates back over one thousand years ago. The use of iron dental implants began sometime around 200 AD in Europe, and the Mayans achieved similar success with seashell nacre around 600 AD (Ratner et al. 2004). But the first attempts to create living tissue replacements outside the body were performed in the early 1970s (Vacanti 2006), when an orthopedic surgeon attempted to produce artificial cartilage by seeding chondrocytes onto small pieces of bone. Since then, there has been enormous progress towards developing the cells (Haynesworth et al. 1992; Takahashi and Yamanaka 2006), scaffold materials (Langer and Folkman 1976; Whang et al. 1998), and biochemical factors (Wang et al. 1990; Jaiswal et al. 1997) that support generation of artificial tissues.

Successful demonstrations of synthetic human implants began with thin, flat structures like skin (Yannas et al. 1982; Heimbach et al. 1988) and cornea (Nishida et al. 2004). Building on these early clinical successes, it was soon discovered that planar constructs could be wrapped around mandrels to produce hollow cylindrical tissues for clinical replacement of tubular structures like the trachea (Macchiarini et al. 2008) and urethra (Raya-Rivera et al. 2011). Researchers have also folded these thin tissues into hollow spherical constructs for bladder replacement (Atala et al. 2006). But despite the clinical successes of 2D and hollow tissues, there have been few reports of solid tissue substitutes that can maintain cellular viability and function post implantation. This is because cells within the interior regions of dense, solid tissues will rapidly die in the absence of efficient vasculature, due to the inability of oxygen and nutrients to rapidly diffuse over distances above 100–200 μm (Kang et al. 2016).

Therefore, there is a critical need to fabricate tissue engineered constructs with innate vascular networks. With biomimetic culture conditions, it is possible to induce de novo vascular growth by seeding endothelial cells in 3D scaffolds (Wang et al. 2015); but this process is not scalable to constructs of clinically relevant dimensions, as cells on the interior regions will die before they have time to mature into vessels, anastomose, and establish a network of fluidic conduits capable of providing convective nutrient transport. By creating fluidic networks – with or without an endothelial lining – within the bulk of these biomaterial scaffolds as part of the initial fabrication process, it is thus possible to prevascularize artificial tissues. Here, we highlight contemporary strategies for the vascularization of 3D printed and engineered tissues. We discuss the advantages and limitations of various fabrication platforms in the field and explore strategies to achieve fluidic integration with the host circulation.

2 Diverse Methods to Produce Macroporous Scaffolds

At their simplest level, the purpose of vascular networks is to overcome the limits of diffusion by supplying routes for convective mass transport throughout the body. Oxygen, nutrients, and waste products must be dynamically exchanged between native tissues and the circulatory system, so that consumed nutrients can be replenished and so waste does not accumulate. In an engineered tissue, the simplest way to achieve this goal is to incorporate macroscopic porosity into a biomaterial scaffold and subject that construct to perfusion culture. 3D hydrogel scaffolds do in fact have micro- or nanoscopic pores, but the size of these voids translates to immensely high fluidic resistance. With such high resistance to flow, subjecting these scaffolds to perfusion may not elicit physiologically relevant convective transport or hemocompatible flows (McGuigan and Sefton 2007).

One method to produce macroporous polymer scaffolds is gas foaming. In this process, alkaline salt particles are first dissolved in a highly concentrated polymer solution. After solvent evaporation, a solid polymer scaffold remains. A chemical reaction occurs when acidic solution is introduced to the system, causing gas to foam through the polymer scaffold and introducing macroporous architecture to the construct (Fig. 1a). Jun and West examined this technique using polyurethaneurea and demonstrated the ability to control pore size and overall porosity by changing salt size and concentration, respectively (Jun and West 2005).

Similar macroporous scaffolds have also been fabricated with a method known as electrospinning, in which a high voltage is used to draw nanoscopic polymer fibers around the circumference of a rotating mandrel. Pham and colleagues studied the influence of perfusion culture on mesenchymal stem cells (MSCs) when seeded on electrospun polycaprolactone discs (Fig. 1b), which were fit into flow cassettes and subjected to flow rates as large as 1 mL/min (Pham et al. 2006). Successful perfusion at this flow rate indicated the macropores were interconnected, thus providing channels for convective flow that present significant fluidic conductance. Furthermore, this model was also used to show that perfusion enhanced MSC infiltration distance by a factor of 5 when compared to static culture. However, the void space of perfused scaffolds filled with matrix secreted by the cells, eventually blocking perfusion.

Gas foaming and electrospinning offer exceptionally high surface area-to-volume ratios for efficient cell seeding and present a wide variety of materials to work with. But the resultant macroporous architectures are stochastically defined by thermodynamic processes. In comparison, traditional 3D printing by melt extrusion is capable of producing macroporous scaffolds of defined, reproducible, and tunable architectures. By melt extruding thermoplastic polymer onto a receiving build platform, 3D scaffolds can be constructed in a point-by-point fashion with submillimeter resolution. However, this modality is limited to materials that will cool and solidify almost instantaneously after extrusion, which is necessary for the printed features to maintain their geometry before the next layer is printed. Using melt extrusion, Trachtenberg and coworkers fabricated macroporous polycaprolactone scaffolds with uniform or gradient pore sizes (Fig. 1c; Trachtenberg et al. 2014). The study

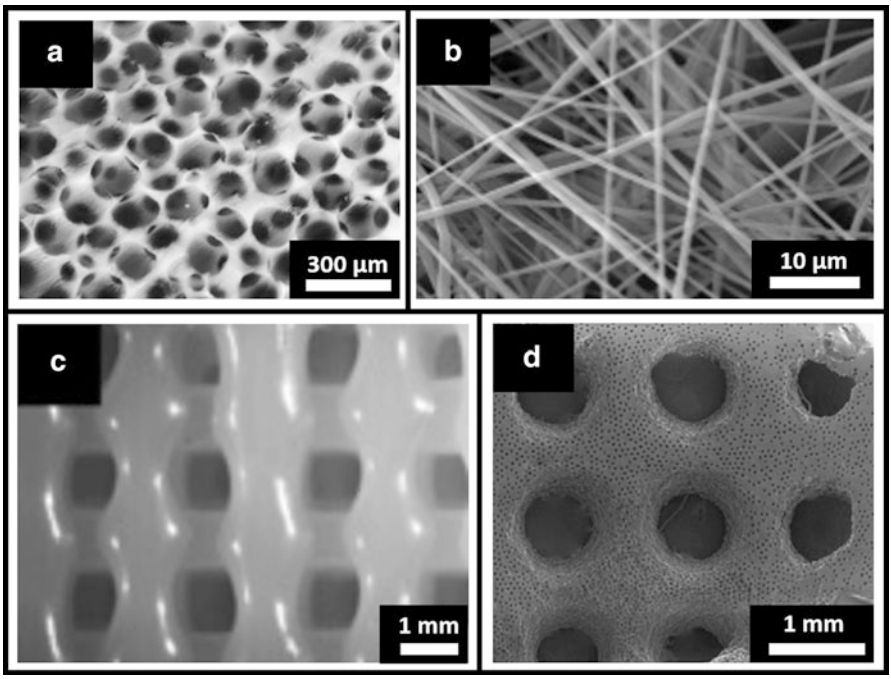

Fig. 1 Macroporous scaffolds to support convective mass transport. Stochastically defined porous architectures generated by (**a**) gas foaming (Costantini et al. 2016) and (**b**) electrospinning (Pham et al. 2006). User-defined pore lattices defined by (**c**) melt extrusion (Trachtenberg et al. 2014) and (**d**) photolithography (Bryant et al. 2007) (Adapted with permission from Elsevier (**a**, **d**), the American Chemical Society (**b**), and John Wiley and Sons (**c**))

rigorously explores how pore size and overall porosity can be reproducibly controlled by extrusion pressure, programmed spacing between extruded filaments, and printing speed.

Macroporous scaffolds with defined architectures can also be fabricated by photolithography, in which user-defined light patterns are used to selectively crosslink polymer solutions into rigid hydrogel features. To generate light patterns, a device with patterned holes of arbitrary shape – known as a photomask – is used to transmit light only in predetermined geometries. Liu Tsang and colleagues used this technology to construct hexagonal lattice architectures, whose large void fraction was intended to minimize barriers to nutrient transport during cell culture (Liu Tsang et al. 2007). Hepatocytes were encapsulated within the lattice struts by mixing them into the photosensitive polymer solution prior to crosslinking. The constructs were fit into a customized flow chamber, and it was shown that perfusion culture – supported by the large pores – elicited a higher magnitude of liver-specific albumin secretion and urea synthesis when compared to static controls.

An example of a similar macroporous scaffold built using photolithography can be seen in Fig. 1d. Here, a photomask was used to define circular pores of 500 µm

diameter (Bryant et al. 2007). The material was patterned around removable plastic microspheres of 62 μm, yielding even smaller pores within the lattice struts to complement the macroporous geometry. Pores introduced by microsphere templating were previously demonstrated to improve cell migration (Stachowiak et al. 2005); however, the overall hydraulic conductivity was not examined.

3 Production of Defined 2D Networks Using Replica Molding

Despite the utility of macroporous scaffolds in cellular assays, porosity is different from vascularization. Macropores are not self-contained to a tubular network geometry and do not possess unifying fluidic ports to facilitate controlled perfusion of a vascularized tissue construct. For artificial tissues intended for clinical implantation, discrete access ports must exist so that fluidic connection with the host circulatory system can be made, and so that circulating blood does not leak out into the bodily cavities.

Replica molding is a commonly used technique to fabricate defined vascular networks with unifying fluidic ports. In essence, replica molding of vascular networks involves three distinct stages: fabricating a negative (i.e., complementary) mold of the desired vascular network, casting a biomaterial matrix around the mold, and then removing the mold. Using cylindrical needles as a molding tools, Chrobak and coworkers were able to fabricate single 100 μm channels within collagen matrix (Fig. 2a – left) (Chrobak et al. 2006). Collagen proteins contain cell-binding peptide domains, which enabled endothelial cells to adhere to the vessel walls and spread to form confluent monolayers (Fig. 2a – right). The putative vessels were shown to exhibit strong barrier function and low leukocyte adhesion, which could be reversed by the introduction of inflammatory agonists like histamine. This reversible behavior is characteristic of native vessels, illustrating the physiological relevance of this vascular model.

This needle-molding technique was further developed by Hasan and coworkers, who used three concentric needles as their replica mold to produce a tri-layered structure (Hasan et al. 2015). Here, a single glass capillary of about 1.5 mm diameter was first used as a mold for silicone casting. Two concentric hypodermic needles were then inserted into the resulting channel, with outer diameters chosen so that there was void space between each element. A suspension of fibroblasts in gelatin methacrylate solution was pipetted within the outer void space and was photocrosslinked into a rigid hydrogel by bulk irradiation to form an annular tissue that mimics vascular adventitia. The large needle is removed, and the process is repeated with smooth muscle cell-laden gelatin to form a second annular tissue, mimicking the tunica media. The last needle is removed, and endothelial cells are seeded around the luminal wall. Thus, the three major layers of native vascular tissue were recapitulated in one device while also maintaining a patent lumen for perfusion (Fig. 2b). While these single vessels may likely be useful for studying fundamental vascular biology, it is difficult to imagine scaling this process to build vascularized tissue constructs of clinically relevant dimensions.

A different replica molding technique known as soft lithography is better suited to produce vascular networks of clinical dimension and biomimetic geometry. To make a network of channels using soft lithography, standard photolithography (described earlier) is first used to pattern positive, rigid features on a silicon wafer. A polymer solution of hydrogel or silicone precursor (known as prepolymer) is then cast against these positive features (Fig. 2c – left), leaving negative, trench-like features imprinted on an otherwise solid structure. This trench-containing structure is then bonded to flat slab of similar material, yielding fluidically sealed vascular networks (Fig. 2c – right).

Cabodi and associates used soft lithography to form a rectilinear lattice of perfusable channels with a single pair of fluidic ports and channel diameters as small as 25 μm (Fig. 2d; Cabodi et al. 2005). Importantly, this luminal diameter approaches that of native capillaries, which typically range between 5 and 10 μm.

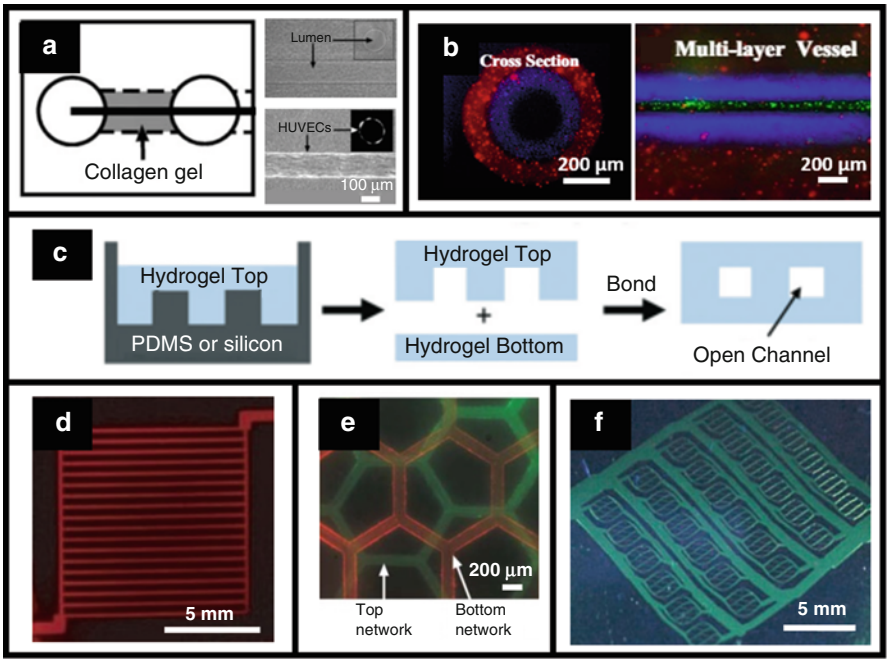

Fig. 2 Replica molding to produce defined fluidic networks. (**a**) Removal of a metal needle from a collagen hydrogel cast yields a single lumen that supports endothelial cell monolayer formation (Chrobak et al. 2006). (**b**) Molding over concentric needles provides discrete layer heterogeneity (red cells, blue cells) within a perfusable conduit. Green fluorescent bead perfusion demonstrates vessel patency (Hasan et al. 2015). (**c**) Simplified schematic of soft lithography (Kinstlinger and Miller 2016). (**d**) A simple rectilinear lattice, made perfusable by unifying fluidic ports (Cabodi et al. 2005). (**e**) Two independent networks combined within a single construct (Golden and Tien 2007). (**f**) Hierarchical branching and diameter reductions within a fluidic network, made perfusable by unifying fluidic ports (King et al. 2004) (Adapted with permission from Elsevier (**a**), the Royal Society of Chemistry (**c**, **e**), the American Chemical Society (**d**), and John Wiley and Sons (**f**))

For construct molding, gelation of alginate polymer solution was induced by simple addition of calcium chloride. Importantly, this ionic crosslinking mechanism is amenable to bulk cellular encapsulation. To achieve bonding between the two gel pieces, surface crosslinks were chelated with sodium citrate, pieces were brought into contact, and crosslinks were reestablished by reintroducing calcium chloride solution.

This process has also been extended to produce channel networks within hydrogels in a 3D fashion. By perfusing warm gelatin through a 2D network – formed via soft lithography – and allowing the gelatin to cool into a hydrogel, Golden and colleagues produced thermoreversible filament networks for subsequent hydrogel encapsulation (Golden and Tien 2007). These gelatin networks were stacked, and collagen was cast around them. After warming the entire system to melt the gelatin structures and subsequently flushing them with PBS, the result was a 3D fluidic network contained within a biocompatible, cell-adhesive matrix (Fig. 2e). The authors went further to demonstrate the formation of composite gel networks, in which the fluidic channels were bound by collagen on top and fibrin on bottom. Despite the 3D nature of these fluidic networks, their clinical relevance is limited due to lack of unifying fluidic ports. For each layer of stacked gelatin networks, a new inlet/outlet pair is introduced to the resultant construct. This would make it difficult to manually access the entire fluidic network, limiting the potential of this technique to be utilized for in vitro studies and clinical implantation.

Soft lithography also provides a means to recapitulate the hierarchical nature of vascular branching that is present in native tissues. Avoiding the need for expensive biological gels, King and coworkers fabricated a hierarchical fluidic network by casting melted poly(DL-lactic-*co*-glycolide) pellets around poly(dimethyl siloxane) (PDMS) molds, and laminating the top and bottom components of the channel via thermal bonding instead of chemical crosslinking as described earlier (King et al. 2004). They were able to demonstrate fluidic networks with fractal-like branching and channel diameter reductions (Fig. 2f), which is a characteristic of native vascular systems that helps blood to quickly reach the entire body, reduce energy loss through viscous dissipation (Razavi et al. 2014), and provide alternate circulatory paths in the event of clotting.

4 Extrusion of Solid Materials to Define Physical Boundaries of Hollow Vessels

Soft lithography, while able to generate near-capillary sized vessel networks, is largely limited to in vitro studies where the resultant chip-like devices can be restrained by microscope stages or mechanical chambers. There have been few – if any – reports of vascularized devices produced by soft lithography that go on to be implanted in animal studies. Thus, there is need to transition from vascular chips to monolithic vascular tissues. The search for prevascularized tissue engineered constructs has recently taken form in extrusion-based methods, where free-standing scaffolds can be fabricated, physically manipulated, and perfused.

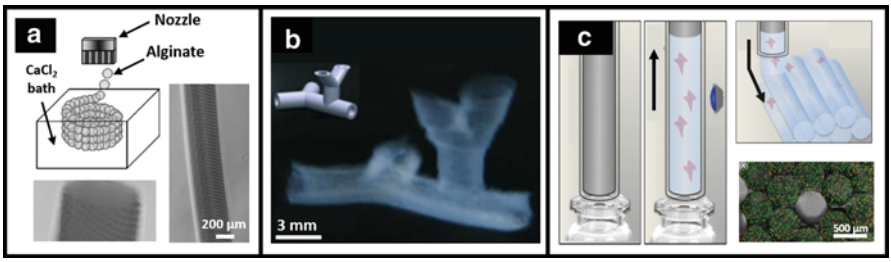

Fig. 3 Extrusion of solid materials to define vascular walls. (**a**) Hollow conduits fabricated by inkjet printing of alginate into calcium chloride solution (Nakamura et al. 2008). (**b**) 3D, branching vessels fabricated by alginate inkjet printing (Christensen et al. 2015). (**c**) Photocrosslinking of cell-laden gelatin filaments. Filaments can be hexagonally stacked to yield a hollow tube (Bertassoni et al. 2014a) (Adapted with permission from the Society for Imaging Science and Technology (**a**), John Wiley and Sons (**b**), and the Institute of Physics (**c**))

The fabrication of monolithic vascular conduits has been repeatedly explored with an extrusion technology known as inkjet printing. These printers use the same extrusion method as their 2D namesake counterparts, where droplets of material are individually released onto a substrate to build a 2D pattern or 3D structure. In 2008, Nakamura and colleagues demonstrated the ability of inkjet printing to construct biocompatible vascular conduits (Nakamura et al. 2008). Droplets of alginate polymer solution were dropped into a bath of aqueous calcium chloride, which induced ionic crosslinking of the droplets into rigid microgel beads with diameters as small as 10 µm. By using microgel beads to plot an annulus pattern, and then superimposing this structure with additional equivalent layers, it was possible to fabricate a hollow tubular construct with 200 µm inner diameter (Fig. 3a). The group went further to show that HeLa cells could be incorporated into the alginate solution prior to gelation, allowing for the fabrication of viable cell-laden tubes (Nishiyama et al. 2009).

A near-identical procedure was outlined by Christensen and associates, but with substantially higher architectural complexity. In this report, inkjet printing of alginate microgels was used to fabricate vascular-like structures with branching in all three dimensions (Fig. 3b), which, as discussed earlier, is a critical component of native vascular systems (Christensen et al. 2015). Furthermore, fibroblasts were incorporated into the alginate solution prior to printing, and 90% viability was observed within the walls of these constructs 24 h after printing.

In an alternative extrusion technique, Jakab and coworkers demonstrated that multicellular aggregates could be used as a bioink for 3D printing (Jakab et al. 2008). To form the aggregates, cells were first centrifuged to a dense pellet and aspirated into a capillary. The compacted cellular filament was then extruded, and a custom device cleaved the material into cylinders of 500 µm height and diameter. A variety of cell types were used to form these bioink aggregates: ovary, smooth muscle, cardiac, and endothelial. Remarkably, it was observed that cellular cylinders could spontaneously round into spherical aggregates, and they were thusly re-aspirated into a capillary for extrusion patterning. Fusion of pellets was observed after printing

in an annular geometry, which allowed for subsequent fabrication of 3D tubes and hollow, branched architectures.

Streamlining this approach in 2014, Bertassoni and coworkers removed the need for point-by-point fabrication by extruding and assembling cell-laden hydrogel filaments into hollow tubes (Bertassoni et al. 2014a). 3T3 fibroblasts were first suspended in a solution of gelatin methacrylate and ultraviolet-absorbing photoinitiator. The mixture was then aspirated into the 500 μm diameter glass capillary of a commercial bioprinter. The entire capillary was irradiated with ultraviolet light, causing free-radical decomposition of the photoinitiator compound, which further reacts by crosslinking gelatin's methacrylate groups to yield a cell-laden hydrogel filament. Mechanical extrusion was used to layer filaments in a hexagonally packed architecture, thus enabling the fabrication of hollow vessels (Fig. 3c).

5 Coaxial Extrusion Improves the Speed and Ease of Vessel Fabrication

While inkjet printing has made great progress towards achieving free-standing vascular mimics, it is difficult to establish fluidic connections with these soft, compliant structures. Unable to be properly manipulated, these constructs are largely incompatible with perfusion culture and in vivo integration. Alternatively, researchers have explored coaxial extrusion printing, which directly produces hollow filaments that maintain structural integrity.

This technique has been rigorously described by Zhang and colleagues. First, two syringe tips of different diameters are concentrically fit together to form a single extrusion nozzle with two discrete openings. By simultaneously extruding a jacket of negatively charged alginate solution around an inner solution of calcium chloride, a hollow hydrogel filament is created as divalent calcium ions crosslink the alginate polymer (Zhang et al. 2015). Custom coaxial tips allowed tuning of outer diameter, inner diameter, and wall thickness, achieving patent fluidic channels as small as 700 μm in diameter.

To demonstrate use as a novel bioprinting modality, human smooth muscle cells were incorporated into the alginate solution prior to extrusion and crosslinking. Low post-fabrication viability (33%) was attributed to extrusion shear stress, but the encapsulated cells exhibited substantial proliferation and smooth muscle cell-specific matrix deposition after 6 weeks in static culture. Interestingly, matrix deposition was found most abundantly near the lumen and circumference of the hollow filaments, suggesting higher activity within these regions of greater oxygen and nutrient supply. Although perfusion culture was not explored, it was shown that these conduits could support media perfusion without leakage after connection to a flexible needle was made with the help of surgical clips. With this method, it was possible to achieve arbitrary pattern complexity in 2D, as seen by the branching and zigzag vessels shown in Fig. 4a. It is important to note that the overall construct dimensions presented here would require prohibitively long fabrication times if attempted with inkjet printing.

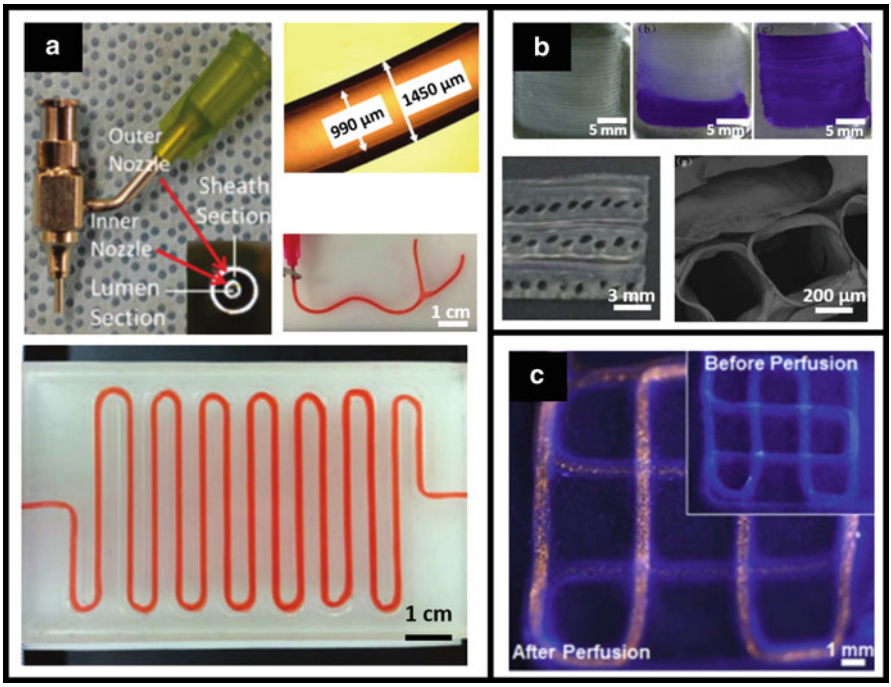

Fig. 4 Coaxial extrusion of hollow vessels. (**a**) Clockwise from *top left*: photograph of a coaxial extrusion nozzle; micrograph demonstrating the hollow nature of extruded filaments; a branched filament; a large (>1 cm) vessel printed with complex 2D geometry (Zhang et al. 2015). (**b**) Fusion of hollow filaments into complex structures. *Top panel*: perfusion of a continuous lumen within a 2D sheet. *Bottom panel*: filaments stacked and fused in 3D, but without unifying perfusion ports (Gao et al. 2015). (**c**) A single hollow filament stacked atop itself in a lattice conformation, which permits continuous 3D perfusion of yellow fluorescent beads (Jia et al. 2016) (Adapted with permission from the Royal Society of Chemistry (**a**) and Elsevier (**b**, **c**))

Using the same coaxial extrusion technique described above, Gao and coworkers explored the capacity for 3D stacking afforded by hollow alginate filaments (Gao et al. 2015). In this report, it was first noted that the inner core of calcium chloride solution was unable to fully crosslink the outer alginate jacket during printing, as rapid gelation prevented complete radial diffusion of the calcium ions. But leveraging this phenomenon provided a means of 2D and 3D filament fusion, as filaments extruded side-by-side could be crosslinked together by immersion in a calcium chloride bath. Single hollow filaments were first fused into 2D sheets of square and spiral geometries, and perfusion of colored dye was used to demonstrate persistence of a continuous 900 µm lumen throughout the sheets (Fig. 4b – top panel). Multiple hollow filaments were then used to build 3D structures in a layer-by-layer process (Fig. 4b – bottom panel); however, perfusion of the entire structure was not possible due to the lack of unifying fluidic ports. In actuality, these 3D structures more closely resemble macroporous scaffolds than vascularized constructs, as the multitude of constituent vessels is not fluidically connected.

In a study by Jia and colleagues, multiple improvements to coaxial extrusion printing were explored (Jia et al. 2016). While previous studies used pure alginate to form hollow hydrogel filaments, here the bioink was formulated as a blend of alginate, gelatin methacrylate, 4-arm poly(ethylene glycol)-tetra-acrylate (PEGTA), and ultraviolet-absorbing photoinitiator. During coaxial extrusion, the rapid ionic crosslinking between alginate and calcium chloride provided temporary structural integrity. The filament networks were then bulk irradiated with ultraviolet light to crosslink the gelatin and PEGTA and immersed in chelating agent to remove the alginate's ionic crosslinks. The incorporation of gelatin provided cell-adhesive peptide domains for cell encapsulation studies, and the presence of PEGTA helped maintain structural integrity after removing alginate. PEGTA forms covalent crosslinks, which were chosen in favor of alginate's ionic crosslinks due to their more permanent nature. While the presence of alginate contributed to enhanced mechanical stability during printing, alginate is bioinert and was thusly chosen to be removed so that cells could more easily spread and proliferate in their artificial matrix (Tamayol et al. 2015)

By utilizing this bioactive hydrogel formulation, it was possible to examine the behavior and function of encapsulated cells beyond simple viability assays. Initially, encapsulated endothelial cells and MSCs were sparsely distributed within the walls of the printed hollow filaments. It was shown that after 21 days in culture these cells were not only able to spread, migrate, and proliferate within this bioactive matrix, but the two cell types had also colocalized. Heterotypic interactions between endothelial cells and MSC support endothelial function (Jeon et al. 2014), and these results thusly demonstrate the potential of the described bioink blend to yield biologically relevant vessels. It was also shown that a single hollow filament could be extruded atop itself in a stacked lattice architecture (Fig. 4c), allowing perfusion of fluorescent beads through a continuous, 3D vessel.

6 Extrusion of Sacrificial Filaments Provides Intricate Control Over Vascular Geometry

At this point, each of the fabrication modalities discussed herein have sought to fabricate vascular networks by focusing on the construction of physical boundaries to define hollow lumen. Recently, an alternative approach known as sacrificial templating has emerged. In this family of techniques, materials are patterned as self-supporting structures that mimic the desired vascular geometry. A bulk material is then cast around this template, and the template is removed to yield a 3D construct with internal fluidic networks (Fig. 5a). By patterning geometries that reflect a vascular network instead of the physical boundaries that define one, researchers have been able to construct vascular networks with intricate curvature and hierarchical branching that are otherwise difficult to produce.

Hydrogels are perhaps the most well-studied sacrificial materials, as their chemistries can be tuned to contain reversible, noncovalent crosslinks that facilitate liquefaction and elution. Bertassoni and colleagues have demonstrated sacrificial templating of agarose (Bertassoni et al. 2014b), which gels via reversible

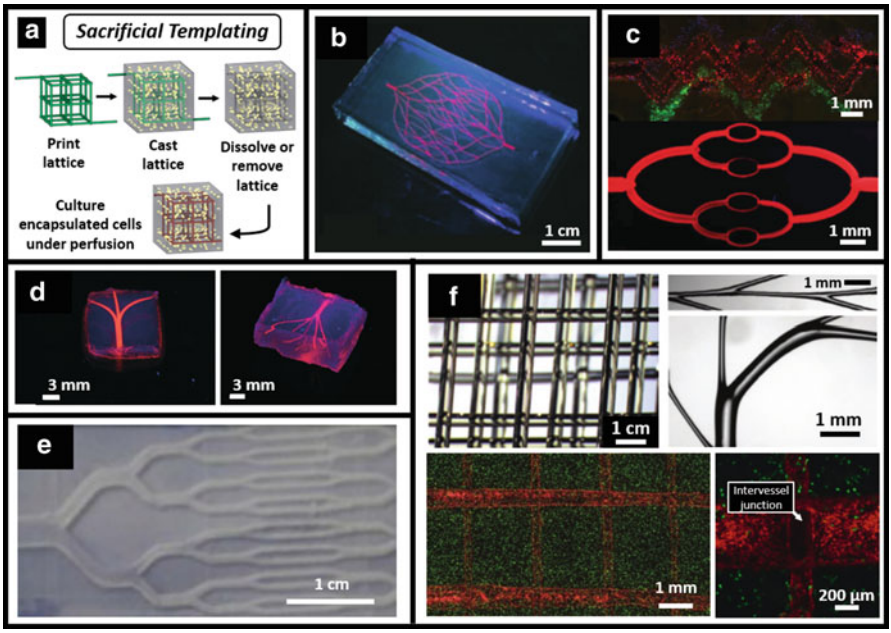

Fig. 5 Sacrificial templating permits fabrication of vascular networks with highly tunable architectures. (**a**) Schematized process of sacrificial templating (Miller et al. 2012). (**b**) Sacrificial templating of Pluronic (Wu et al. 2011). (**c**) Another example of sacrificial templating of Pluronic (Kolesky et al. 2014). (**d**) Sacrificial templating of agarose (Bertassoni et al. 2014b) and (**e**) poly (vinyl) alcohol (Jeffries et al. 2014). (**f**) Clockwise from *top left*: a 3D lattice template made from carbohydrate glass; branching and curvature within a template lattice; endothelial cell (*red*) monolayer formation within a fibroblast-laden gel (*green*) after template removal; a patent, 3D intervessel junction (Miller et al. 2012) (Adapted with permission from John Wiley and Sons (**b**, **c**, **e**) and the Royal Society of Chemistry (**d**))

temperature-dependent chain entanglement (Horinaka et al. 2014). In this study, a piston was first used to aspirate molten agarose into a capillary, where the temperature was cooled below 32 °C to permit gelation. The rigid filaments were then extruded into branching and 3D lattice architectures, with individual diameters as small as 250 μm. Hydrogels of various chemical nature were cast around these templates, and the template filaments were then removed via manual pulling or light vacuum. This report highlights the chemical versatility of sacrificial templating, as four unique photocrosslinkable polymers – of synthetic and natural origin – were shown to support template casting. With the help of discrete fluidic ports, network perfusion with red fluorescent microbeads was clearly demonstrated (Fig. 5d). Furthermore, it was shown that the presence of microchannels enhanced not only the viability of bulk-encapsulated 3T3 fibroblasts but also osteogenic differentiation.

Pluronic® polymer has also been studied as a sacrificial template for the fabrication of vascularized tissues. Pluronic is a water-soluble polymer that undergoes a thermally reversible gelation process when dissolved in preparations above its

critical micelle concentration (Bohorquez et al. 1999). Transition temperatures range between 4 °C and 10 °C and are a function of polymer concentration. At temperatures slightly above this transition point, Pluronic behaves as a hydrogel with shear-thinning behavior. This unique property enables it to not only be extruded via pressure-driven mechanisms but to also retain structural rigidity after extrusion from a printer nozzle. These printed network patterns can be subsequently casted in an acellular or cell-laden hydrogel. By lowering the temperature below Pluronic's transition point, the printed filaments can be flushed with water or cell culture media leaving behind a perfusable fluidic network. Hence, sacrificial filaments are often referred to as fugitive ink.

In a fabrication scheme realized by Wu and colleagues, fugitive Pluronic ink is extruded directly into a reservoir of photosensitive matrix, providing a physical support for the printed filament network (Wu et al. 2011). As the extrusion nozzle physically translates through the reservoir matrix, it tears a path which is filled in by a photosensitive filler liquid residing atop the support matrix. When the desired geometry is fully printed, the entire system is exposed to ultraviolet light. This crosslinks the support and filler materials together, fully encasing the Pluronic ink. Lowering the system temperature below Pluronic's transition point facilitates liquefaction and flushing of the printed template, yielding 2D vascular networks. Near-capillary sized channels of 18 μm diameter were able to be fabricated, and a network of highly intricate curves and branches was successfully perfused through unifying fluidic ports (Fig. 5b).

This method of sacrificial Pluronic templating was further expanded by the same group to generate 3D fluidic networks within a monolithic cell-laden hydrogel (Kolesky et al. 2014). In a layer-by-layer process, fugitive Pluronic ink was templated concurrently with fibroblast-laden gelatin filaments (Fig. 5c). The entire system was cast with acellular GelMA hydrogel, and the Pluronic template was flushed by lowering the ambient temperature to yield microchannels with diameters down to 150 μm. This printing method was shown to be compatible with immortalized 10T1/2 fibroblasts and primary human neonatal dermal fibroblasts, as demonstrated by post-fabrication viability and proliferation. By simultaneously patterning cells and vasculature within a bulk acellular environment, it was possible to maintain cellular proximity to nutrient supply conduits within a large, monolithic tissue construct. It is important to note that this method enabled fabrication of 3D vascular networks with unifying fluidic ports, facilitating easy template removal and network perfusion.

In a subsequent report by this group, sacrificial templating of Pluronic was used to study longitudinal perfusion culture of a thick (>1 cm^3), vascularized tissue construct (Kolesky et al. 2016). Here, lattice networks of MSC-laden gelatin and acellular Pluronic were first printed in an interpenetrating fashion. The system was cast with fibroblast-laden gelatin, the fugitive template was flushed, and endothelial cells were seeded within the resulting fluidic network. This process enabled successful integration of parenchyma, stroma, and endothelium, which represents a near-complete anatomical unit cell (excluding nerves and lymphatics). Not only did encapsulated cells maintain viability over 6 weeks in perfusion culture, but osteogenic differentiation of the parenchyma was observed after 30 days when supplemented with bone morphogenetic protein 2. It was found that osteogenic expression was inversely

proportional to nearest vessel distance, indicating that perfusion culture provided this thick tissue with enhanced oxygen and nutrient supplies.

Beyond hydrogels, extrusion of carbohydrate glass has also been used to pattern sacrificial templates for tissue vascularization. Using sucrose, glucose, and dextran, Miller and colleagues were able to find an optimal stoichiometric ratio that simultaneously supported aqueous melt extrusion and rapid vitrification (Miller et al. 2012). The resulting filaments were sufficiently rigid to support overhanging features when patterned in a 3D lattice, permitting the fabrication of curves and branches of continuously tunable diameters between 150 and 750 μm (Fig. 5f). To tune filament diameters during printing, nozzle translation speed was modulated. Aside from providing architectural tunability, the templates were also shown to support hydrogel casting through a wide variety of gelation mechanisms: agarose – chain entanglement; alginate – ionic interactions; PEGDA – photopolymerization; fibrin – enzyme activity; Matrigel – protein precipitation.

The sacrificial template geometry was designed to provide unifying fluidic access ports, enabling various perfusion studies after template dissolution in aqueous medium. Importantly, the templated networks supported pulsatile human blood flow, with each microchannel and 3D intervessel junction receiving a visible fraction of the perfusate. It is critical to note that an arbitrarily designed network geometry may produce redundant branches with no pressure drop across their length, resulting in low flow rates or none at all. Remarkably, endothelial cells seeded within the lumens of casted fibrin gels were observed to adhere, form confluent monolayers, and undergo angiogenic sprouting into the bulk after 9 days in perfusion culture. Furthermore, encapsulated fibroblasts were found to exhibit a characteristic radius of viability around each channel, which demonstrates the need for angiogenic sprouting and multiscale anastomosis in tissues of clinically relevant dimensions.

As noted previously, one advantage of sacrificial templating is that it supports casting of a wide variety of materials. In a study by Jeffries and associates, melt extruded poly(vinyl alcohol) (PVA) (Jeffries et al. 2014) templates were used as a vascular mold for electrospun polydioxanone (PDO). PVA is extremely water soluble, which enabled quick dissolution from the PDO cast to yield a hollow fluidic network (Fig. 5e). Due to the fibrous nature of electrospun scaffolds, suturing of vascular constructs was explored. Suture strength was measured by inserting a suture and pulling both ends of the thread away from the construct until rupture. Strengths comparable to commonly sutured polycaprolactone were observed, and anastomosis between channels was demonstrated by directly suturing two PDO conduits. This strategy offers potential for in vivo integration of artificial fluidic networks, but the electrospinning process does not currently allow for cellular seeding within the bulk.

7 Stereolithography as a Single-Step Fabrication Platform for 3D Vessel Networks

Empowered by replica molding, direct extrusion, and sacrificial templating, tissue engineers have fabricated perfusable constructs of intricate geometry that support endothelial cell seeding and bulk cell encapsulation. But these fabrication schemes

are time-consuming and often require several intermediate processing steps, limiting their throughput to single construct experiments. Stereolithography (SLA) is a 3D printing technology that promises to dramatically increase the production rates of vascularized tissues, while also maintaining high spatial resolution and a relatively unrestricted design space.

Like extrusion-based methods, SLA builds 3D structures in a layer-by-layer process. However, instead of directly extruding material onto a build platform, SLA uses emitted light patterns to selectively crosslink photosensitive polymer solutions into hydrogel structures of user-defined geometries. The patterned light layers can either be rasterized by a laser spot using mirror galvanometers, or generated using a digital micromirror device (DMD) in a process known as projection stereolithography. DMDs use an array of microscopic mirrors – each able to toggle between an on or off state – to reflect user-defined patterns towards a substrate (Fig. 6a). DMDs are often referred to as dynamic photomasks, because they achieve the same light-patterning function as physical photomasks but can dynamically change their spatial configurations.

In one early demonstration of SLA, Arcaute and coworkers used an ultraviolet laser to photocrosslink PEG-based polymer solutions into 3D hydrogel conduits (Arcaute et al. 2006). Structures with multiple parallel lumens were fabricated, as were constructs of clinically relevant dimensions (1 × 1 × 5 cm) containing a single inlet that bifurcates twice in different planes to generate four unique outlets (Fig. 6d). Despite this unique ability to achieve truly unrestricted 3D geometry, channel diameters were limited to 500 μm. This limitation is largely governed by the laser

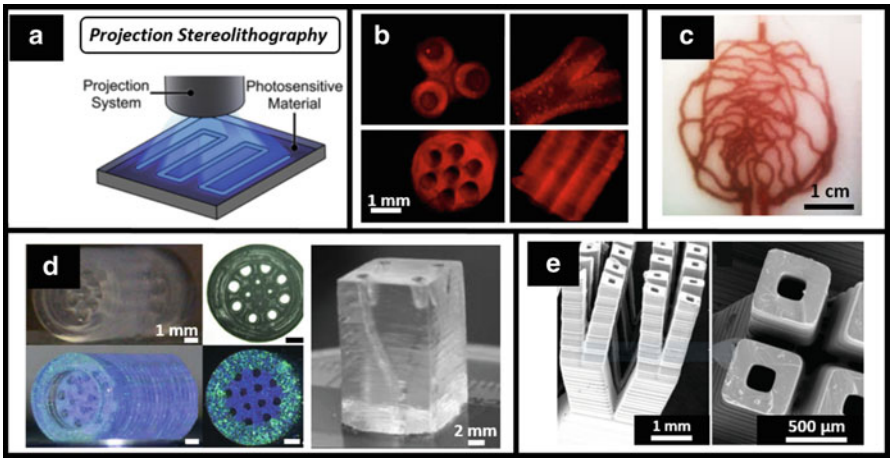

Fig. 6 Single-step fabrication of intricate fluidic networks using SLA. (**a**) Schematic of projection SLA (Miller and Burdick 2016). (**b**) Two different vessel architectures printed using projection SLA (Suri et al. 2011). (**c**) Perfusion of hemoglobin through a laser SLA-printed replica of human retinal vasculature (Ghassemi et al. 2015). (**d**) Multilumen conduits and a branched 3D network printed with laser SLA (Arcaute et al. 2006). (**e**) Hierarchical branching of 224 μm diameter channels, fabricated by a commercially available projection SLA printer (Schüller-Ravoo et al. 2014) (Adapted with permission from SPIE (**c**) and John Wiley and Sons (**e**))

spot size, which was 250 μm in this particular study. Perfusion through the resultant fluidic networks was not performed; however, it was clear from visual inspection that the channels remained patent. Human dermal fibroblasts were then incorporated into the initial polymer solution to investigate cytotoxic effects of the SLA process. The cells were found to maintain >87% viability 24 h after fabrication, indicating that their SLA process could provide vascular networks within cell-laden tissue constructs.

Similar vascular geometries where fabricated by Suri and colleagues, choosing to use projection SLA in lieu of the laser-based method (Suri et al. 2011). Here, acrylated hyaluronic acid was used as the photosensitive polymer. By incorporating a free radical quenching agent into the initial polymer solution, it was possible to reduce off-target crosslinking and fabricate single-layer channels (i.e., wells) with diameters as small as 150 μm. However, the observed resolution improvement did not translate during multilayer 3D printing, where the minimum printable diameter of multilumen and branched geometries was 500 μm (Fig. 6b).

In the past decade, the SLA process has been formalized into commercial 3D printers for hobbyists, industry, and research. In work by Ghassemi and colleagues, a commercial laser SLA printer was used to build fluidic network geometries derived from optical micrographs of human retinal vasculature (Ghassemi et al. 2015). Hemoglobin solutions were perfused through the networks, and every branch successfully filled (Fig. 6c). These results suggest a possible solution to an open question in vascular tissue engineering: what is the ideal vascular architecture? In its simplest form, an ideal vascular network is one in which each branch receives enough convective mass transport to support proximal cell metabolism. Native vascular systems are capable of pruning redundant, nonflowing branches (Lenard et al. 2015), and thus future designs of artificial fluidic networks may benefit from mimicking geometries derived from in vivo imaging. Although the authors eliminated branches with diameters less than 450 μm from the final 3D design – due to resolution constraints – complete perfusion was still observed. Unfortunately, the commercial SLA printer required use of a proprietary, nonbiocompatible polymer, so it would not be feasible to encapsulate cells within the bulk of these constructs to study perfusion culture.

In other studies, commercial SLA printers have been used to fabricate vascularized structures within biocompatible materials. Using a novel polycarbonate derivative with an industrial, projection SLA printer, Schüller-Ravoo and colleagues demonstrated production of channels with internal diameters of 224 μm (Schüller-Ravoo et al. 2014). These microchannels were hierarchically designed to reflect an idealized capillary network, where a single outlet undergoes sequential branching generations to obtain a large number of daughter vessels (Fig. 6e). These vessels anastomose into one outlet, yielding a high-density, perfusable network of microvessels that was shown to support systolic-mimicking fluid pressure of 120 mmHg. Endothelial cells could adhere to and proliferate on the printed material; however, viable cell encapsulation would need to be demonstrated in future work in order to indicate utility as a vascular tissue scaffold.

8 Advanced Fabrication Technologies

Between replica molding, extrusion, and light-based printing technologies, tissue engineers have a wide variety of platforms to choose from when building vascularized constructs. But researchers are still searching for new ways to improve these methods and devise new technologies, *as there is currently no unifying platform that can fabricate vessels with unrestricted 3D geometric control and with lumen dimensions that mirror the multiscale nature of native vasculature.*

In work by Meyer and colleagues, a variation of SLA known as multiphoton polymerization was used to generate branching vessels of near-capillary-sized diameter (Fig. 7a; Meyer et al. 2012). Multiphoton polymerization produces 3D structures by crosslinking photosensitive polymer solutions with a laser, much like laser SLA. But in this technique, the exciting photons have approximately twice the wavelength of the photoinitiator's maximum absorption peak. The nature of this absorption phenomenon confines the free-radical crosslinking reaction to a small 3D volume at the focal plane of the laser beam (Oheim et al. 2006), yielding comparatively higher resolution than traditional SLA. Remarkably, 18 μm lumen diameters and 5 μm wall thicknesses were achieved in this report. But multiphoton polymerization is hindered by comparatively slow fabrication speeds, limiting its dimensional scalability.

With respect to the goal of unrestricted geometric complexity, researchers have turned to some very nontraditional methods to build structures that curve and branch in multiple planes. In one report, Bhattacharjee and colleagues used a novel extrusion method to fabricate multiscale vessel networks with hierarchical branching in numerous planes (Bhattacharjee et al. 2015). To support these branching, overhanging features in 3D space, crosslinkable polymers were directly extruded into a slurry of 7 μm hydrogel particles. This support material fluidizes from a solid state at a threshold shear stress, providing physical support to the extruded material while concurrently allowing the extrusion nozzle to travel to various 3D coordinates. After crosslinking the printed material into a monolithic construct, the structure could be retrieved by water immersion, which disperses the granular slurry. This technique can be used to print PDMS and collagen, which crosslink through chemical reactions, and polymers like PVA, which can be modified to be photosensitive. Impressively small lumen diameters of about 200 μm were printed; however, it can be seen from Fig. 7b that branching junctions are not fluidically sealed and would certainly leak under perfusion.

Choosing a different supporting slurry of 50 μm gelatin particles, Hinton and colleagues fabricated similar branching structures (Fig. 7c – left) and achieved perfusion without leakage (Fig. 7c – right) (Hinton et al. 2015). The supporting gelatin medium was removed by simply raising the ambient temperature above gelatin's melting temperature, yielding overhanging vessel walls that supported convective flow. Despite the merit of nonleaking geometry, vessel diameters were on the order of millimeters; refining the technique to yield higher spatial resolution would be needed to improve its utility in the field.

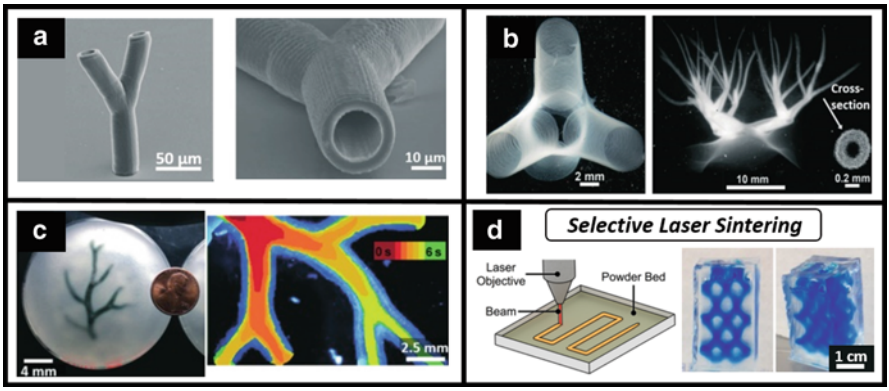

Fig. 7 Advanced technologies to support unrestricted geometric control in 3D space. (**a**) Multi-photon polymerization of a branched, capillary-scale vessel (Meyer et al. 2012). (**b**) Hierarchical branching of hollow vessels by extrusion of solid material into granular slurry (Bhattacharjee et al. 2015). (**c**) *Left*: a branched fluidic network formed by reversible embedding in granular support. *Right*: successful perfusion of the resulting vessels (Hinton et al. 2015). (**d**) *Left*: schematized printing process of SLS (Miller and Burdick 2016). *Right*: a branching 3D network fabricated by SLS, made perfusable by unifying fluidic ports (Kinstlinger and Miller 2016) (Adapted with permission from MDPI (**a**), American Association for the Advancement of Science (**b**, **c**), and Public Library of Science (**d**))

An alternative support-based printing method known as selective laser sintering (SLS) can also be used to fabricate branching vessel networks with unrestricted 3D geometry. In SLS, 3D parts are built in a layer-by-layer fashion as a focused laser beam traces 2D patterns into a thin layer of powder (Fig. 7d – left). The powder absorbs the electromagnetic radiation, melts, and fuses into a solid, connected structure. The key advantage of SLS is its ability to build overhanging 3D features that would otherwise collapse if printed in air using traditional extrusion methods. Overhanging features can be sintered atop the unfused powder of previous layers, which acts as a support material much like the microparticle slurries discussed above.

In a study by Kinstlinger and associates, polycaprolactone powder was sintered into a 3D lattice that served as a water-soluble, sacrificial template for hydrogel casting (Kinstlinger et al. 2016). The resulting hydrogel constructs contained fluidic network with overhanging bifurcations in 3D space, and perfusion of blue dye was made possible by a unifying inlet and outlet (Fig. 7d – right). Although not explicitly outlined in this report, this technique would likely be compatible with cell encapsulation for tissue engineering: cells could simply be incorporated into the hydrogel prepolymer solution prior to crosslinking around the SLS-printed template. Furthermore, the ability to fabricate multiple templates at once – each of arbitrary dimensions – enables SLS to function in a high-throughput, geometrically scalable fashion.

9 Multiscale Vasculature Produced by Endothelial Matrix Invasion

The techniques discussed so far have clearly demonstrated achievement of cell-laden tissue constructs that contain intricate, 3D vascular geometries. But the lumens of native capillaries range between 5 and 10 μm in diameter and building fluidic networks of this scale still remains elusive. Instead of further refining 3D printing technologies to achieve capillary-sized vessels, researchers are increasingly relying on the innate developmental abilities of endothelial cells to achieve this task.

In work by Zheng and colleagues, tubular endothelial monolayers were shown to produce angiogenic sprouts into a surrounding collagen matrix in the presence of perfused vascular endothelial growth factor (VEGF) (Zheng et al. 2012). While the diameters of these sprouts were not directly characterized, it was clear from visual inspection that they were smaller than 50 μm. This ability to induce angiogenic sprouting from microfabricated channels may serve as a multiscale link between capillary- and arteriole-sized vessels. However, perfusion of angiogenic factors concurrently led to disorganization of intercellular junctions and diminished barrier function as observed by perfusion of high-molecular weight fluorescent molecules. Interestingly, encapsulation of human brain vascular pericytes, which are known to synthesize VEGF (Dore-Duffy et al. 2006), within the collagen bulk enabled simultaneous maintenance of barrier function and angiogenic sprouting (Fig. 8a) without the presence of exogeneous growth factors.

Nugyen and coworkers further explored the use of chemokine gradients and found that robust angiogenic sprouting of ~50 μm diameter vessels could support anastomosis between two prefabricated channels (Nguyen et al. 2013). In this study, needle molding of collagen was used to initially form two parallel channels of 400 μm diameter (Fig. 8d – left). One channel was seeded with endothelial cells to achieve a confluent monolayer, while the other channel remained acellular and supported axial perfusion of an angiogenic cocktail that included VEGF. By diffusing across the collagen matrix, the resulting chemotactic gradient induced directional angiogenesis towards the perfusion channel in the form of fully lumenized, multicellular sprouts that exhibited clear apical-basal polarity. Remarkably, the growing sprouts breached the chemokine source channel after 1 week, forming continuous, near-capillary-sized lumens between the two prefabricated channels. 3 μm red fluorescent beads were perfused through the parent channel to visualize flow path, and the beads were indeed able to travel to the factor source channel with no interstitial leakage (Fig. 8d – right).

In addition to exogenous growth factors and pericyte interactions, the effects of fluidic stress on angiogenic sprouting have also been explored. In native vascular systems, circulation exerts shear stress on the endothelium via two mechanisms: luminal flow, which shears the cells across their flat, apical surfaces, and transmural flow, which shears the membrane at intercellular junctions as fluid exists the vessel wall into the interstitium. By seeding endothelial monolayers within needle-molded

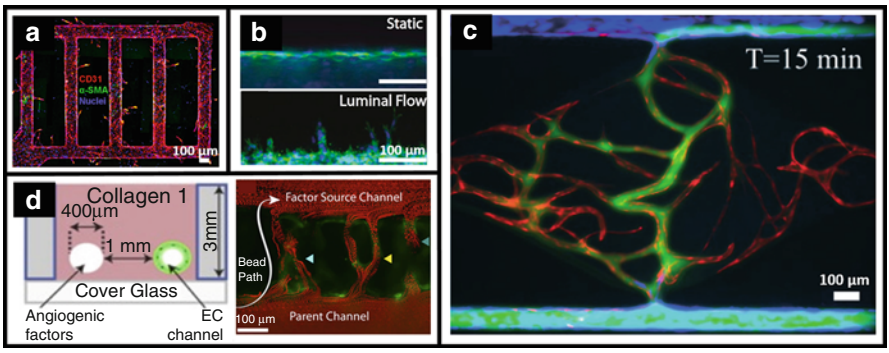

Fig. 8 In vitro models demonstrate the utility of angiogenesis and vasculogenesis in the production of multiscale vasculature. (**a**) Angiogenic sprouting into a bulk collagen gel, induced by pericyte co-culture. Staining for CD31 – a prominent endothelial marker – provides visualization of sprouts within the otherwise dark collagen bulk (Zheng et al. 2012). (**b**) Angiogenic sprouting induced by the shear stress associated with luminal perfusion (Galie et al. 2014). (**c**) Multiscale anastomosis between two patterned microvessels (*blue*) and a capillary network formed through vasculogenesis of encapsulated endothelial cells (*red*). Minimal leakage is confirmed by perfusion of 70 kDa fluorophore (*green*) (Wang et al. 2015). (**d**) Multiscale anastomosis between an endothelial cell-seeded vessel and a channel perfused with chemotactic factors. Absence of leakage confirmed by red fluorescent bead perfusion (Nguyen et al. 2013) (Adapted with permission from the National Academy of Sciences (**a**, **b**, **d**) and the Royal Society of Chemistry (**c**))

collagen channels, Galie and colleagues clearly demonstrated that a threshold shear stress exists, above which cells will sprout regardless of whether the shear is presented by luminal flow (Fig. 8b) or transmural flow (Galie et al. 2014). Thus, integration of chemotaxis and mechanotransduction may prove useful in future efforts to fabricate multiscale vasculature within tissue engineered constructs.

As opposed to angiogenesis, vasculogenesis has also been leveraged to establish multiscale vessel networks. Whereas angiogenesis is the process by which new vessels sprout from preexisting ones, vasculogenesis occurs as lumenized tubules (i.e., capillaries) develop de novo from individual endothelial cells (Risau 1997). In work by Wang and coworkers, this process of vasculogenesis was realized by exposing an endothelial cell-laden fibrin gel to chemotactic gradients from two flanking microchannels (Wang et al. 2015). The containing device was made from dense, hydrophobic silicone so diffusive transport of the chemokines from the patterned microchannels into the gel region was made possible by two 50 μm pores. Developing tubules were observable by day 3, at which point the prepatterned microchannels were seeded with endothelial cells to investigate the system's potential for anastomosis through the tunnel. A mature capillary network had formed within the gel region by day 12, and minimal leakage of perfused 70 kDa fluorophore confirmed anastomosis between the lumenized capillaries and patterned microchannels (Fig. 8c).

Using angiogenic and vasculogenic platforms, researchers have established multiscale vascular networks that may support the mass transport needs of artificial tissues. However, these demonstrations of multiscale anastomosis were performed in lab-on-a-chip platforms, which have limited potential for in vivo integration.

10 Progress Towards Integration In Vivo

By fabricating vascular networks within engineered tissues, we ultimately hope to provide cells with vessels for exchange of oxygen, nutrients, and waste after implantation. This requires not only the presence of internal fluidic networks but also a mechanism by which these vessels can integrate with the host circulatory system. So far, host integration has been demonstrated by two primary mechanisms: spontaneous, cell-driven anastomosis, and surgical anastomosis.

Cell-driven anastomosis between implanted vascular networks and the host circulatory system has been demonstrated by Kim and colleagues (2016). In this study, endothelial cells were first encapsulated within a dual-layered hydrogel of chitosan-lactide copolymer. The cell-containing layer was chemically crosslinked using an inorganic reagent, yielding a relatively soft gel that provided a suitable environment for vasculogenesis and construct remodeling. To provide physical support during surgical implantation, the cell-laden hydrogel was laminated to a chemically identical, acellular hydrogel that was instead crosslinked using ultraviolet light to provide a relatively stiff environment. The engineered tissue constructs were cultured for 5 days prior to implantation, giving time for tubule networks to develop through vasculogenesis.

To assess potential for anastomosis in mice, the vascularized gels were physically placed between termini of ligated and transected femoral arteries without direct suturing. Laser Doppler imaging was then used to observe hind limb circulation over time. It was found that circulation rates were significantly higher in animals that received gel implants with microvascular networks (Fig. 9a), thus indicating that the implanted vessels had spontaneously anastomosed with femoral collateral vessels to reestablish hind limb circulation. However, these fluidic networks had no discrete inlets and outlets, and so it is possible that circulating blood was also concurrently leaking into the body cavities.

As we and others have previously demonstrated, fluidically tight connections between artificial and host vascular systems can be achieved by surgical methods as opposed to spontaneous, cell-driven events. In this report, an artificial vascular network was first fabricated by casting PDMS around a sacrificial template of carbohydrate glass (Sooppan et al. 2016). The sacrificial template was designed to have unifying fluidic ports, providing the resultant PDMS construct with discrete connections for surgical anastomosis. This procedure was relatively simple: rat femoral arteries were ligated, transected, and manually inserted – without suturing – into the inlet and outlet ports of the artificial vascular network. After unclamping the femoral artery to introduce circulatory perfusion (Fig. 9b), laser Doppler imaging confirmed network patency and pulsatile flow. It is also important to note that no signs of leakage were observed. The dimensional tolerance between the PDMS channel and femoral artery was apparently small enough to ensure tight fluidic connection, which is a critical finding because many hydrogels used by researchers today would fracture under the stress of suture threading.

While Sooppan and colleagues used acellular PDMS constructs to study circulatory perfusion over 3 h, a different group has used cell-laden, biodegradable gels to study

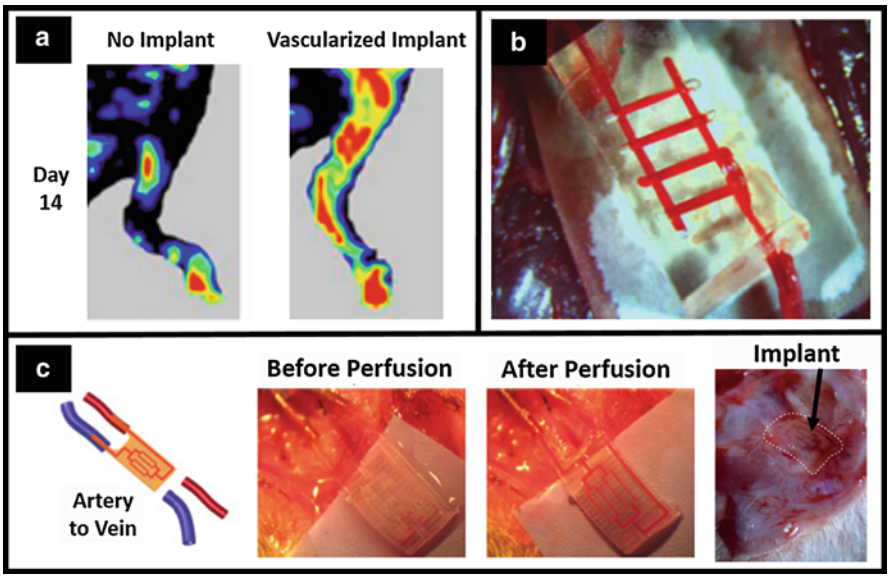

Fig. 9 Spontaneous and surgical anastomosis between artificial fluidic networks and host vasculature. (**a**) Spontaneous anastomosis between implanted endothelial tubule networks and femoral collateral vessels supported mouse hind limb recirculation (as seen here by laser Doppler imaging) after femoral artery transection (Kim et al. 2016). (**b**) After severing a rat femoral artery, circulation was reestablished through a fluidic network formed from sacrificial templating of carbohydrate glass (Sooppan et al. 2016). (**c**) A rat model arteriovenous shunt was established using a fluidic network fabricated via sequential layering of molds, each fabricated in a single soft lithography process (Zhang et al. 2016). Note the immediately successful perfusion and the lack of visible inflammation after 1 week in vivo. Due to the nature of in vivo imaging, scale bars were difficult to obtain (Adapted with permission from the American Chemical Society (**a**))

the biological behavior of exogeneous tissues after surgical anastomosis. In a report by Zhang and coworkers, vascular networks were first fabricated within a rigid scaffold of citric acid-based polymer (Zhang et al. 2016). Cardiomyocytes were then suspended in fibrin or Matrigel prepolymer solution and encapsulated around the fluidic network so that the parenchymal response to in vivo integration could be assessed. The geometry of the bulk construct was cleverly designed to have protruding inlet and outlet regions to facilitate direct cannulation within the femoral artery and vein, respectively (Fig. 9c – left). Fluidic connections were secured with cyanoacrylate tissue glue, in contrast to the manual press fit technique described earlier.

Circulatory perfusion through the vascular construct (Fig. 9c – middle) persisted for 1 week without visible signs of leakage, and with 85% of lumen remaining clot-free. This finding is consistent with previous literature, which suggest that some citric acid-based polymers exhibit antithrombotic properties (Kibbe et al. 2010). In vascular networks preseeded with endothelial cells, angiogenic sprouting into the hydrogel bulk was also observed after 1 week of circulatory perfusion. Furthermore, not only were encapsulated cardiomyocytes able to maintain their physiologic

phenotype – as evidenced by troponin T expression – but they could survive without eliciting visible signs of inflammation (Fig. 9c – right).

11 Conclusions

Presently, researchers seeking to endow their artificial tissues with vascular networks have a wide variety of fabrication platforms to choose from. These methods are well-suited to provide simple in vitro platforms and in vivo grafts, but there currently exists no unifying technology that can fabricate perfusable networks with unrestricted geometric control that contain vessels spanning from capillary- to artery-sized diameters. Looking forward, it may be possible to merge several methods to achieve this goal. One could imagine angiogenic sprouting between laser-sintered vessels in hydrogel, simultaneously yielding vasculature of intricate, scalable geometries, that is multiscale in nature. But as vascularized tissue constructs evolve, it is important to reconsider the primary goal of vascular tissue engineering: enhanced mass transport within 3D volumes. We can borrow vessel designs from clinical imaging data, but perhaps there exists some ideal network geometry – unrealized by nature – that could provide nutrient and waste exchange at supra-physiological rates. Bioinspired approaches have certainly led to enormous medical achievements in recent years, but we must also aim to transcend what is possible within the confines of human biology.

References

Arcaute K, Mann BK, Wicker RB (2006) Stereolithography of three-dimensional bioactive poly (ethylene glycol) constructs with encapsulated cells. Ann Biomed Eng 34:1429–1441. https://doi.org/10.1007/s10439-006-9156-y

Atala A, Bauer SB, Soker S, Yoo JJ, Retik AB (2006) Tissue-engineered autologous bladders for patients needing cystoplasty. Lancet 367:1241–1246. https://doi.org/10.1016/S0140-6736(06)68438-9

Bertassoni L, Cardoso JC, Manoharan V, Cristino AL, Bhise NS, Araujo WA, Zorlutuna P, Vrana NE, Ghaemmaghami AM, Dokmeci MR, Khademhosseini A (2014a) Direct-write bioprinting of cell-laden methacrylated gelatin hydrogels. Biofabrication 6:24105. https://doi.org/10.1088/1758-5082/6/2/024105

Bertassoni L, Cecconi M, Manoharan V, Nikkhah M, Hjortnaes J, Cristino AL, Barabaschi G, Demarchi D, Dokmeci MR, Yang Y, Khademhosseini A (2014b) Hydrogel bioprinted microchannel networks for vascularization of tissue engineering constructs. Lab Chip 14:2202–2211. https://doi.org/10.1039/c4lc00030g

Bhattacharjee T, Zehnder SM, Rowe KG, Jain S, Nixon RM, Sawyer WG, Angelini TE (2015) Writing in the granular gel medium. Sci Adv 1:e1500655. https://doi.org/10.1126/sciadv.1500655

Bohorquez M, Koch C, Trygstad T, Pandit N (1999) A study of the temperature-dependent micellization of Pluronic F127. J Colloid Interface Sci 216:34–40. https://doi.org/10.1006/jcis.1999.6273

Bryant SJ, Cuy JL, Hauch KD, Ratner BD (2007) Photo-patterning of porous hydrogels for tissue engineering. Biomaterials 28:2978–2986. https://doi.org/10.1016/j.biomaterials.2006.11.033

Cabodi M, Choi NW, Gleghorn JP, Lee CSD, Bonassar LJ, Stroock AD (2005) A microfluidic biomaterial. J Am Chem Soc 127:13788–13789. https://doi.org/10.1021/ja054820t

Christensen K, Xu C, Chai W, Zhang Z, Fu J, Huang Y (2015) Freeform inkjet printing of cellular structures with bifurcations. Biotechnol Bioeng 112:1047–1055. https://doi.org/10.1002/bit.25501

Chrobak KM, Potter DR, Tien J (2006) Formation of perfused, functional microvascular tubes in vitro. Microvasc Res 71:185–196. https://doi.org/10.1016/j.mvr.2006.02.005

Costantini M, Colosi C, Mozetic P, Jaroszewicz J, Tosato A, Rainer A, Trombetta M, Wojciech Ś, Dentini M, Barbetta A (2016) Correlation between porous texture and cell seeding efficiency of gas foaming and microfluidic foaming scaffolds. Mater Sci Eng C 62:668–677. https://doi.org/10.1016/j.msec.2016.02.010

Dore-Duffy P, Katychev A, Wang X, Van Buren E (2006) CNS microvascular pericytes exhibit multipotential stem cell activity. J Cereb Blood Flow Metab 26:613–624. https://doi.org/10.1038/sj.jcbfm.9600272

Galie PA, Nguyen D-HT, Choi CK, Cohen DM, Janmey PA, Chen CS (2014) Fluid shear stress threshold regulates angiogenic sprouting. Proc Natl Acad Sci U S A 111:7968–7973. https://doi.org/10.1073/pnas.1310842111

Gao Q, He Y, Fu J, Liu A, Ma L (2015) Coaxial nozzle-assisted 3D bioprinting with built-in microchannels for nutrients delivery. Biomaterials 61:203–215. https://doi.org/10.1016/j.biomaterials.2015.05.031

Ghassemi P, Wang J, Melchiorri AJ, Ramella-Roman JC, Mathews SA, Coburn JC, Sorg BS, Chen Y, Pfefer TJ (2015) Rapid prototyping of biomimetic vascular phantoms for hyperspectral reflectance imaging. J Biomed Opt 20:121312. https://doi.org/10.1117/1.JBO.20.12.121312

Golden AP, Tien J (2007) Fabrication of microfluidic hydrogels using molded gelatin as a sacrificial element. Lab Chip 7:720–725. https://doi.org/10.1039/b618409j

Hasan A, Paul A, Memic A, Khademhosseini A (2015) A multilayered microfluidic blood vessel-like structure. Biomed Microdevices 17:9993. https://doi.org/10.1007/s10544-015-9993-2

Haynesworth SE, Goshima J, Goldberg VM, Caplan AI (1992) Characterization of cells with osteogenic potential from human marrow. Bone 13:81–88. https://doi.org/10.1016/8756-3282(92)90364-3

Heimbach D, Luterman A, Burke J, Cram A, Herndon D, Hunt J, Jordan M, McManus W, Solem L, Warden G (1988) Artificial dermis for major burns. A multi-center randomized clinical trial. Ann Surg 208:313–320. https://doi.org/10.1097/00000658-198809000-00008

Hinton TJ, Jallerat Q, Palchesko RN, Park JH, Grodzicki MS, Shue H, Ramadan MH, Hudson AR, Feinberg AW (2015) Three-dimensional printing of complex biological structures by freeform reversible embedding of suspended hydrogels. Sci Adv 1:1–10. https://doi.org/10.1126/sciadv.1500758

Horinaka J ichi, Urabayashi Y, Wang X, Takigawa T (2014) Molecular weight between entanglements for κ- and ι-carrageenans in an ionic liquid. Int J Biol Macromol 69:416–419. https://doi.org/10.1016/j.ijbiomac.2014.05.076

Jaiswal N, Haynesworth SE, Caplan AI, Bruder SP (1997) Osteogenic differentiation of purified, culture-expanded human mesenchymal stem cells in vitro. J Cell Biochem 64:295–312. https://doi.org/10.1002/(sici)1097-4644(199702)64:2<295::aid-jcb12>3.0.co;2-i

Jakab K, Norotte C, Damon B, Marga F, Neagu A, Besch-Williford CL, Kachurin A, Church KH, Park H, Mironov V, Markwald R, Vunjak-Novakovic G, Forgacs G (2008) Tissue engineering by self-assembly of cells printed into topologically defined structures. Tissue Eng Part A 14:413–421. https://doi.org/10.1089/ten.2007.0173

Jeffries EM, Nakamura S, Lee K-W, Clampffer J, Ijima H, Wang Y (2014) Micropatterning electrospun scaffolds to create intrinsic vascular networks. Macromol Biosci 14:1514–1520. https://doi.org/10.1002/mabi.201400306

Jeon JS, Bersini S, Whisler JA, Chen MB, Dubini G, Charest JL, Moretti M, Kamm RD (2014) Generation of 3D functional microvascular networks with human mesenchymal stem cells in microfluidic systems. Integr Biol 6:555–563. https://doi.org/10.1039/C3IB40267C

Jia W, Gungor-Ozkerim PS, Zhang YS, Yue K, Zhu K, Liu W, Pi Q, Byambaa B, Dokmeci MR, Shin SR, Khademhosseini A (2016) Direct 3D bioprinting of perfusable vascular constructs using a blend bioink. Biomaterials 106:58–68. https://doi.org/10.1016/j.biomaterials.2016.07.038

Jun H-W, West JL (2005) Endothelialization of microporous YIGSR/PEG-modified polyurethaneurea. Tissue Eng 11:1133–1140. https://doi.org/10.1089/ten.2005.11.1133

Kang H-W, Lee SJ, Ko IK, Kengla C, Yoo JJ, Atala A (2016) A 3D bioprinting system to produce human-scale tissue constructs with structural integrity. Nat Biotechnol. https://doi.org/10.1038/nbt.3413

Kibbe MR, Martinez J, Popowich DA, Kapadia MR, Ahanchi SS, Aalami OO, Jiang Q, Webb AR, Yang J, Carroll T, Ameer GA (2010) Citric acid-based elastomers provide a biocompatible interface for vascular grafts. J Biomed Mater Res A 93:314–324. https://doi.org/10.1002/jbm.a.32537

Kim S, Kawai T, Wang D, Yang Y (2016) Engineering a dual-layer chitosan-lactide hydrogel to create endothelial cell aggregate-induced microvascular networks in vitro and increase blood perfusion in vivo. ACS Appl Mater Interfaces 8:19245–19255. https://doi.org/10.1021/acsami.6b04431

King KR, Wang CCJ, Kaazempur-Mofrad MR, Vacanti JP, Borenstein JT (2004) Biodegradable microfluids. Adv Mater 16:2007–2012. https://doi.org/10.1002/adma.200306522

Kinstlinger IS, Miller J (2016) 3D-printed fluidic networks as vasculature for engineered tissue. Lab Chip 16:2025–2043. https://doi.org/10.1039/C6LC00193A

Kinstlinger IS, Bastian A, Paulsen SJ, Hwang DH, Ta AH, Yalacki DR, Schmidt T, Miller JS (2016) Open-Source Selective Laser Sintering (OpenSLS) of nylon and biocompatible polycaprolactone. PLoS One 11:1–25. https://doi.org/10.1371/journal.pone.0147399

Kolesky DB, Truby RL, Gladman AS, Busbee TA, Homan KA, Lewis JA (2014) 3D bioprinting of vascularized, heterogeneous cell-laden tissue constructs. Adv Mater 26:3124–3130. https://doi.org/10.1002/adma.201305506

Kolesky DB, Homan KA, Skylar-Scott MA, Lewis JA (2016) Three-dimensional bioprinting of thick vascularized tissues. Proc Natl Acad Sci U S A 201521342. https://doi.org/10.1073/pnas.1521342113

Langer R, Folkman J (1976) Polymers for the sustained release of proteins and other macromolecules. Nature 263:797–800

Lenard A, Daetwyler S, Betz C, Ellertsdottir E, Belting HG, Huisken J, Affolter M (2015) Endothelial cell self-fusion during vascular pruning. PLoS Biol 13:1–25. https://doi.org/10.1371/journal.pbio.1002126

Liu Tsang V, Chen AA, Cho LM, Jadin KD, Sah RL, DeLong S, West JL, Bhatia SN (2007) Fabrication of 3D hepatic tissues by additive photopatterning of cellular hydrogels. FASEB J 21:790–801. https://doi.org/10.1096/fj.06-7117com

Macchiarini P, Jungebluth P, Go T, Asnaghi MA, Rees LE, Cogan TA, Dodson A, Martorell J, Bellini S, Parnigotto PP, Dickinson SC, Hollander AP, Mantero S, Conconi MT, Birchall MA (2008) Clinical transplantation of a tissue-engineered airway. Lancet 372:2023–2030. https://doi.org/10.1016/S0140-6736(08)61598-6

McGuigan AP, Sefton MV (2007) The influence of biomaterials on endothelial cell thrombogenicity. Biomaterials 28:2547–2571. https://doi.org/10.1016/j.biomaterials.2007.01.039

Meyer W, Engelhardt S, Novosel E, Elling B, Wegener M, Krüger H (2012) Soft polymers for building up small and smallest blood supplying systems by stereolithography. J Funct Biomater 3:257–268. https://doi.org/10.3390/jfb3020257

Miller JS, Burdick JA (2016) Editorial: special issue on 3D printing of biomaterials. ACS Biomater Sci Eng 2:1658–1661. https://doi.org/10.1021/acsbiomaterials.6b00566

Miller JS, Stevens KR, Yang MT, Baker BM, Nguyen D-HT, Cohen DM, Toro E, Chen AA, Galie PA, Yu X, Chaturvedi R, Bhatia SN, Chen CS (2012) Rapid casting of patterned vascular networks for perfusable engineered three-dimensional tissues. Nat Mater 11:768–774. https://doi.org/10.1038/nmat3357

Nakamura M, Nishiyama Y, Henmi C, Iwanaga S, Nakagawa H, Yamaguchi K, Akita K, Mochizuki S, Takiura K (2008) Ink jet three-dimensional digital fabrication for biological tissue manufacturing: analysis of alginate microgel beads produced by ink jet droplets for three dimensional tissue fabrication. J Imaging Sci Technol 52:1–15. https://doi.org/10.2352/J.ImagingSci.Technol

Nguyen D-HT, Stapleton SC, Yang MT, Cha SS, Choi CK, Galie PA, Chen CS (2013) Biomimetic model to reconstitute angiogenic sprouting morphogenesis in vitro. Proc Natl Acad Sci U S A 110:6712–6717. https://doi.org/10.1073/pnas.1221526110

Nishida K, Yamato M, Hayashida Y, Watanabe K, Yamamoto K, Adachi E, Nagai S, Kikuchi A, Maeda N, Watanabe H, Okano T, Tano Y (2004) Corneal reconstruction with tissue-engineered cell sheets composed of autologous oral mucosal epithelium. N Engl J Med 351:1187–1196. https://doi.org/10.1056/NEJMoa040455

Nishiyama Y, Nakamura M, Henmi C, Yamaguchi K, Mochizuki S, Nakagawa H, Takiura K (2009) Development of a three-dimensional bioprinter: construction of cell supporting structures using hydrogel and state-of-the-art inkjet technology. J Biomech Eng 131:35001. https://doi.org/10.1115/1.3002759

Oheim M, Michael DJ, Geisbauer M, Madsen D, Chow RH (2006) Principles of two-photon excitation fluorescence microscopy and other nonlinear imaging approaches. Adv Drug Deliv Rev 58:788–808. https://doi.org/10.1016/j.addr.2006.07.005

Pham QP, Sharma U, Mikos AG (2006) Electrospun poly (ε-caprolactone) microfiber and multilayer nanofiber/microfiber scaffolds: characterization of scaffolds and measurement of cellular infiltration. Biomacromolecules 7:2796–2805. https://doi.org/10.1021/bm060680j

Ratner B, Hoffman A, Schoen F, Lemons J (2004) Biomaterials science: an introduction to materials in medicine, 2nd edn. Academic, Cambridge

Raya-Rivera A, Esquiliano DR, Yoo JJ, Lopez-Bayghen E, Soker S, Atala A (2011) Tissue-engineered autologous urethras for patients who need reconstruction: an observational study. Lancet 377:1175–1182. https://doi.org/10.1016/S0140-6736(10)62354-9

Razavi MS, Shirani E, Salimpour MR, Kassab GS (2014) Constructal law of vascular trees for facilitation of flow. PLoS One 9:e116260. https://doi.org/10.1371/journal.pone.0116260

Risau W (1997) Mechanisms of angiogenesis. Nature 386:671–684

Schüller-Ravoo S, Zant E, Feijen J, Grijpma DW (2014) Preparation of a designed poly(trimethylene carbonate) microvascular network by stereolithography. Adv Healthc Mater 3:2004–2011. https://doi.org/10.1002/adhm.201400363

Sooppan R, Paulsen SJ, Han J, Ta AH, Dinh P, Gaffey AC, Venkataraman C, Trubelja A, Hung G, Miller JS, Atluri P (2016) In vivo anastomosis and perfusion of a three-dimensionally-printed construct containing microchannel networks. Tissue Eng Part C Methods 22. https://doi.org/10.1089/ten.tec.2015.0239

Stachowiak AN, Bershteyn A, Tzatzalos E, Irvine DJ (2005) Bioactive hydrogels with an ordered cellular structure combine interconnected macroporosity and robust mechanical properties. Adv Mater 17:399–403. https://doi.org/10.1002/adma.200400507

Suri S, Han L-H, Zhang W, Singh A, Chen S, Schmidt CE (2011) Solid freeform fabrication of designer scaffolds of hyaluronic acid for nerve tissue engineering. Biomed Microdevices 13:983–993. https://doi.org/10.1007/s10544-011-9568-9

Takahashi K, Yamanaka S (2006) Induction of pluripotent stem cells from mouse embryonic and adult fibroblast cultures by defined factors. Cell 126:663–676. https://doi.org/10.1016/j.cell.2006.07.024

Tamayol A, Najafabadi AH, Aliakbarian B, Arab-Tehrany E, Akbari M, Annabi N, Juncker D, Khademhosseini A (2015) Hydrogel templates for rapid manufacturing of bioactive fibers and 3D constructs. Adv Healthc Mater. https://doi.org/10.1002/adhm.201500492

Trachtenberg JE, Mountziaris PM, Miller JS, Wettergreen M, Kasper FK, Mikos AG (2014) Open-source three-dimensional printing of biodegradable polymer scaffolds for tissue engineering. J Biomed Mater Res A 4326–4335. https://doi.org/10.1002/jbm.a.35108

Vacanti CA (2006) The history of tissue engineering. J Cell Mol Med 10:569–576. https://doi.org/10.1111/j.1582-4934.2006.tb00421.x

Wang EA, Rosen V, D'Alessandro JS, Bauduy M, Cordes P, Harada T, Israel DI, Hewick RM, Kerns KM, LaPan P et al (1990) Recombinant human bone morphogenetic protein induces bone formation. Proc Natl Acad Sci U S A 87:2220–2224. https://doi.org/10.1073/pnas.87.6.2220

Wang X, Phan DTT, George SC, Hughes CCW, Lee AP (2015) Engineering anastomosis between living capillary networks and endothelial cell-lined microfluidic channels. Lab Chip 16:282–290. https://doi.org/10.1039/C5LC01050K

Whang K, Tsai DC, Nam EK, Aitken M, Sprague SM, Patel PK, Healy KE (1998) Ectopic bone formation via rhBMP-2 delivery from porous bioabsorbable polymer scaffolds. J Biomed Mater Res 42:491–499. https://doi.org/10.1002/(SICI)1097-4636(19981215)42:4<491::AID-JBM3>3.0.CO;2-F

Wu W, Deconinck A, Lewis JA (2011) Omnidirectional printing of 3D microvascular networks. Adv Mater 23:178–183. https://doi.org/10.1002/adma.201004625

Yannas V, Burke JF, Orgill DP, Skrabut EM (1982) Wound tissue can utilize a polymeric template to synthesize a functional extension of skin. Science 215:174–176. https://doi.org/10.1126/science.7031899

Zhang Y, Yu Y, Akkouch A, Dababneh A, Dolati F, Ozbolat IT (2015) In vitro study of directly bioprinted perfusable vasculature conduits. Biomater Sci 3:134–143. https://doi.org/10.1039/C4BM00234B

Zhang B, Montgomery M, Chamberlain MD, Ogawa S, Korolj A, Pahnke A, Wells LA, Massé S, Kim J, Reis L, Momen A, Nunes SS, Wheeler AR, Nanthakumar K, Keller G, Sefton MV, Radisic M (2016) Biodegradable scaffold with built-in vasculature for organ-on-a-chip engineering and direct surgical anastomosis. Nat Mater. https://doi.org/10.1038/nmat4570

Zheng Y, Chen J, Craven M, Choi NW, Totorica S, Diaz-Santana A, Kermani P, Hempstead B, Fischbach-Teschl C, López JA, Stroock AD (2012) In vitro microvessels for the study of angiogenesis and thrombosis. Proc Natl Acad Sci U S A 109:9342–9347. https://doi.org/10.1073/pnas.1201240109